Conformational Energy and Configurational Statistics of Polypropylene

U. W. Suter and P. J. Flory*

Department of Chemistry, Stanford University, Stanford, California 94305.
Received June 16, 1975

ABSTRACT: The intramolecular energy of the chain segment $-CH_2CH(CH_3)CH_2CH(CH_3)CH_2-$ has been computed as a function of its conformation, interactions between every pair of atoms being included. Contributions from methyl group rotations and from the skeletal conformation are separable in good approximation. At each conformation, the two methyl groups of the segment were therefore assigned the rotations that minimize the energy. Ten accessible energy domains (minima) are clearly delineated for the meso dyad, and ten for the racemic dyad. Boltzmann averages over the rotation angles for the dyad pair yield mean conformations for each domain. These are well represented by combinations of five states for each bond, these states being located at 15, 50, 70, 105, and −115° as measured from trans in the right- or the left-handed sense, depending on the chirality of the skeletal bond. Statistical weight matrices of order 5 × 5 are formulated, one for the pair of bonds flanking the substituted carbon center and one for the dyad pair between successive substituted centers; the form of the latter matrix depends on the meso or racemic character of the dyad. Three statistical weight parameters are required. They are evaluated as functions of temperature from the partition functions and average energies computed for each of the domains. The parameters thus calculated are in excellent agreement with values deduced from the recent results of Suter, Pucci, and Pino on the stereochemical equilibration of oligomers. Characteristic ratios C_∞ and their temperature coefficients are satisfactorily reproduced within the accuracy that these quantities are known. In contrast to the predictions of the three-state model used heretofore, C_∞ is predicted to be greatest for syndiotactic polypropylene (ca. 11 at 140°C), and to decrease monotonically as the proportion of meso dyads increases, C_∞ for the isotactic chain (ca. 4.2 at 140°C) actually being somewhat smaller than for the atactic chain (ca. 5.5 at 140°C).

Until recently, experimental results on the conformational characteristics of polypropylene were confined principally to chain dimensions of the random coil and their temperature coefficients. Reliable experimental values of these quantities for stereoregular polypropylenes are difficult to obtain owing to the high melting points of these polymers, and hence their insolubility at moderate temperatures. Atactic polypropylenes are readily soluble, but their stereochemical constitution, or tacticity, is not susceptible to accurate determination by methods now available. Experimental evidence pertaining to the spatial configuration, and hence the conformational interactions in polypropylenes, has therefore been somewhat indecisive with respect to predictions deduced from rotational isomeric state theory.[1]

Stereochemical equilibration affords a much more powerful means for evaluating the conformational characteristics of vinyl polymer chains in those instances where this method is applicable.[2,3] Recently, methods for epimerization have been developed and applied to oligomers of polypropylene with results meeting high standards of accuracy.[4,5] Equilibration was established at temperatures in the range 200 to 290°C, and also at −75°C. Additionally, the optical rotations of (4*R*,6*R*)-2,4,6,8-tetramethylnonane and of (4*S*,8*S*)-2,4,6,8,10-pentamethylundecane were measured, for the latter as a function of temperature. These results together with those for the epimerization equilibria were treated successfully using the rotational isomeric state model based on three rotational states. The statistical weights thus evaluated were shown to be consistent with the less accurate results currently available on the dimensions of polypropylene chains.[6]

The three-state model is known to be approximate.[1,3,7] It affords a satisfactory representation of the preferred conformations for both meso (isotactic) and racemic (syndiotactic) dyads, but fails to take proper account of the complexities of the states of higher energy. These latter are represented in the three-state model by conformations falling at compromised locations displaced considerably from the centers of the domains (minima) for the states of higher energy.[1,3,8,9] In view of the accurate experimental results made available by the recent experiments cited above, a more thorough investigation of the conformational energy of polypropylene seemed appropriate.

The first attempts at calculation of the conformational energy of polypropylene addressed the regular conformations (helices and all-trans chains) generated by assigning the same angles of rotation within every repeat unit (comprising two bonds) of the stereoregular chain. Calculations of this nature were carried out by Natta, Corradini, and Ganis[10,11] and by Borisova and Birshtein.[12] The most stable conformations according to these calculations are in good agreement with the conformations found by X-ray diffraction to occur in crystalline isotactic and syndiotactic polypropylene, respectively. Such calculations are not directly applicable to the molecule in a solution or the melt, where it is not constrained to assume a regular conformation. Under these circumstances much greater ranges of conformation are accessible.

Flory, Mark, and Abe[8] formulated a rotational isomeric state scheme for polypropylene largely by inference from the conformational interactions in polymethylene chains.[9] This scheme has been applied to various monosubstituted vinyl polymers as well as to polypropylene. Conformational energies were calculated for 2,4-dimethylpentane in the vicinity of its preferred conformations, this molecule being viewed as a model for a dyad in polypropylene. The methyl groups were treated as structureless (spherical) domains in these calculations. The number of conformational variables was thereby reduced to two, namely, the rotations about the internal skeletal bonds. In addition to the conventional three states, designated trans (t), gauche (g), and gauche bar (ḡ) according to current notation,[13] the occurrence of two energy minima at rotation angles between t and g was recognized on the basis of analysis of models. Trial calculations of chain dimensions were carried out including these two additional states.[14] It was concluded that, within the limits of accuracy of estimates of the energies on the one hand and of experimental results then available on the other, the contributions of these additional states could be accommodated by minor adjustments of the respective statistical weights for t and g states (and combinations there-

of). Accordingly, the three-state scheme was advocated as a basis for treating polypropylene in particular and vinyl polymers of α-olefins in general.

Boyd and Breitling[15] carried out more detailed calculations on 2,4,6-trimethylheptane which may be regarded as the trimeric oligomer of polypropylene. They took full account of interactions between pairs of individual atoms, and of all nine rotation angles inclusive of the rotations of the five methyl groups. Their computational procedure yielded only the minima in the conformational energy; all other features of the energy were ignored. As has been pointed out elsewhere,[1,7] it is necessary to consider the entire energy surface within the range of accessible energies. Identification of rotational isomeric states with minima of energy, without regard for other regions of the surface, does not suffice as a basis for treating the configurational statistics of a chain molecule. This assertion finds demonstration in the present investigation.

It is further to be noted that calculations on the *intramolecular* energy of the trimer, or triad, may not be directly representative of a pair of dyads in a polypropylene chain as it exists in the liquid state, either in solution or in bulk. van der Waals attractions between atoms and groups at or near the two extremities of this sequence may contribute an appreciable lowering of the conformational energy in compact conformations. But for the model compound or the sequence as it occurs in the liquid, this *intramolecular* energy is compensated by a decrease in the *intermolecular* energy of interaction with surrounding molecules or chain segments. Either the attractions between outer parts of the sequence should be omitted from the total energy, or the intermolecular attractions should be included. These complications increase the greater the length of the segment; opportunities for interactions between remote atoms and groups are enhanced and, simultaneously, the interactions with surrounding molecules acquire a greater dependence on conformation. For a shorter sequence, such as a single dyad inclusive of the atoms and groups joined directly to it, these influences are minimal. Intramolecular attractions show relatively small variations with conformation, and intermolecular interactions are likewise approximately independent thereof. Calculations based on longer sequences must therefore be interpreted with caution.

In this paper we present calculations of the conformational energies of dyads in polypropylene with full account of the interactions between all pairs of atoms. The energy thus computed serves as the basis for constructing a rotational isomeric state scheme which may be expected to represent the polypropylene chain with high accuracy.

Conformational Energies

Parameters for the Calculation of Conformational Energies. An intrinsic threefold torsional potential with a barrier of 2.8 kcal mol^{-1} was assigned to each C–C bond.[9] Nonbonded interactions between atoms separated by more than two bonds were calculated using the Lennard-Jones 6–12 pair-potential $E_{ij} = (a_{ij}/r_{ij}^{12}) - (c_{ij}/r_{ij}^{6})$. Atoms were treated individually, the approximation of representing groups by spherical domains being avoided. The London dispersion parameters c_{ij} were calculated according to the Slater–Kirkwood formula using Ketelaar's values[9,16] for the atom polarizabilities α_i and the "effective number of electrons" N_i. The constants a_{ij} were so assigned as to minimize the potentials E_{ij} for a given pair of atoms when r_{ij} is set equal to the sum of the corresponding adjusted van der Waals radii r_i^0.[3,17] The values used are given in Table I.

Bond angle deformation energies were treated in the harmonic approximation $E_\theta = \Sigma\ (k_\theta/2)(\theta - \theta_0)^2$, all bond angles being included in the sum. Following Schachtschneider, Snyder, and Zerbi,[18,19] the θ_0 were assigned tetrahedral values. Interactions between pendant atoms ("two-bond" interactions) were not explicitly considered inasmuch as such interactions are included in the k_θ given in Table I, according to the procedure followed in their evaluation.[18,19] In effect, we assume the contributions to k_θ from these two-bond interactions to be the same for every bond angle of a given type e.g., for all ∠CCC.

Table I
Parameters Used in Energy Calculations

Atom	r_i^0, Å	α_i, Å^3	N_i
C	1.8	0.93	5
H	1.3	0.42	0.9

Interacting pair	$a_{ij} \times 10^{-3}$, kcal mol^{-1} Å^{12}	c_{ij}, kcal mol^{-1} Å^6
C,C	398	366
C,H	57	128
H,H	7.3	47

Bond	Bond length, Å
C–C	1.53
C–H	1.10

Bond angle	k_θ, mdyn Å rad^{-2}	k_θ, kcal mol^{-1} deg^{-2}
∠CCC	1.0	0.044
∠CCH	0.65	0.029
∠HCH	0.55	0.024

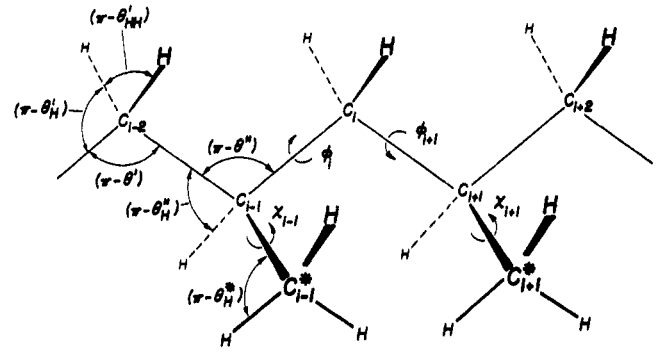

Figure 1. Portion of an isotactic polypropylene chain in the all-trans conformation.

Molecular Geometry. The geometry of the methine group (Figure 1) is fully determined by the angle θ'' if we take all ∠CCC to be equal and treat all ∠CCH likewise.[18] Then $\theta_H'' = \pi - \angle CCH$ is given by

$$(\cos\ \theta_H'')^2 = (1 - 2\cos\ \theta'')/3 \qquad (1)$$

The total deformation energy of the skeletal bond angle ($\pi - \theta''$) calculated using the constants in Table I can be approximated by a single harmonic term $E_{\theta''} \approx A''(\theta'' - \theta_0'')^2$ where A'' is 0.12 kcal mol^{-1}deg^{-2} (400 kcal mol^{-1}rad^{-2}) and $\theta_0'' = 70.5°$.

The geometry of the methylene group is specified by two angles, e.g., θ' and θ_H'. On the assumption that all ∠CCH are equal, $\theta_{HH'} = \pi - \angle HCH$ is given by

$$\cos\ \theta_{HH'} = 1 - 4(\cos\ \theta_H')^2/(1 - \cos\ \theta') \qquad (2)$$

The exact geometry of the methylene group has little influence on the nonbonded interactions of atoms that are separated by more than two bonds in conformations with low energy. For a given value of θ', therefore, $\theta_{HH'}$ was selected to minimize the sum of bond angle deformation energies (which include two-bond interactions; see above). Using the constants in Table I, one finds on this basis that the mutual dependence of the angles is well reproduced by

$$\theta_{HH'} - \theta_{HH,0'} \approx \theta_{H'} - \theta_{H,0'} \approx -0.2(\theta' - \theta_{0'}) \quad (3)$$

In the range $108° \leq (\pi - \theta') \leq 118°$ the total deformation energy of the bond angle $(\pi - \theta')$ can then be approximated by a single harmonic term $E_{\theta'} \approx A' (\theta' - \theta_{0'})^2$ with $A' = 0.025$ kcal mol^{-1}deg^{-2} (80 kcal mol^{-1}rad^{-2}) and $\theta_{0'} = 70.5°$.[20]

The total energy of the chain segment shown in Figure 1 was calculated as a function of θ' and θ'' for the three most populated conformational domains (see below) (meso;tg, racemic;tt, and racemic;gg), the rotation angles φ_i, φ_{i+1}, χ_{i-1}, and χ_{i+1} being adjusted to minimize the conformational energy inclusive of nonbonded interactions between atoms that are separated by more than two bonds for each combination θ',θ''. The conformational energy surfaces thus computed exhibited shallow minima around $\theta' \approx 111°$, $\theta'' \approx 114°$ in each case. The energy increased by 1 kcal mol^{-1} at ca. 109 and 113° for θ'' and ca. 110 and 118° for θ'. These surfaces over θ', θ'' are closely similar for the several states of low energy, apart from uniform displacement of the energy scale. Differences between them vary less than 0.2 kcal mol^{-1} within the stated ranges of θ' and θ''. Numerical calculations confirm that the foregoing conclusions are not conditional on the assignments chosen for the θ_0's and the bond angle force constants, values for which differ considerably[21] from one author to another.

Locations φ_i,φ_{i+1} of the principal minima in the conformational energy calculated for fixed values of θ' and θ'' change little for small alterations in θ' and θ''; at the limits of the ranges stated above for increments in energy up to 1 kcal mol^{-1} the changes do not exceed 15°. The precise locations φ_i,φ_{i+1} of the minima are of little importance; averages over conformational domains surrounding the minima are employed in the following analysis. These averages are less sensitive to the bond angles than the positions of the minima.

The evidence offered by the computations briefly summarized above clearly justifies the procedure followed below of assigning fixed values to the bond angles, the fact notwithstanding that the average values of the bond angles must vary slightly with conformation. The variation is large only for the $\bar{g}\bar{g}$ conformations where we expect the distortion of θ' to resemble that in polyisobutylene, *i.e.*, ca. 12°.[22] Incidence of these conformations is so low as to render them unimportant.

Crystallographic investigations[23-25] on polypropylene indicate values of ca. 114° for both $\pi - \theta'$ and $\pi - \theta''$. This exceeds the result, 111°, calculated above. The experimental bond angles for similar structures suggest $\pi - \theta'' \approx 111°$ (isobutane[26]) and $\pi - \theta' \approx 112°$ (*n*-alkanes[3]), both of which agree satisfactorily with our calculations. Hence, we take $\pi - \theta' = \pi - \theta'' = 112°$ as in earlier studies.[8,9] In keeping with eq 3 we take $\pi - \theta_{H'} = 109°$, and $\pi - \theta_{H}^* = 110°$.

Conformational Energies and Rotational Isomeric States. The conformational energy of a dyad (Figure 1) depends on four rotation angles φ_i, φ_{i+1}, χ_{i-1}, and χ_{i+1}. In order to simplify the representation of $E(\varphi_i,\varphi_{i+1},\chi_{i-1},\chi_{i+1})$ we chose to compute the energy for the values of χ_{i-1} and χ_{i+1} that minimize the energy for each pair of values of the skeletal torsion angles φ_i and φ_{i+1}. Use of energies thus calculated finds justification below. The resulting conformational energy, $E(\varphi_i,\varphi_{i+1})$, being a function of two variables, may then be represented in the customary fashion as contours on the φ_i,φ_{i+1} plane. Figures 2 and 3 show the energy maps thus computed for a "meso" and a "racemic" dyad, respectively, with contours drawn at the indicated intervals of energy in kcal mol^{-1} relative to the tt minimum for the racemic dyad. The energies were calculated at intervals of 10° for φ_i and φ_{i+1} within the range $E \leq 10$ kcal mol^{-1} relative to racemic;tt and at intervals of 20° elsewhere. The minimization of the energy by side-group rotation χ_{i-1} and χ_{i+1} was performed using a well-known iterative algorithm.[27]

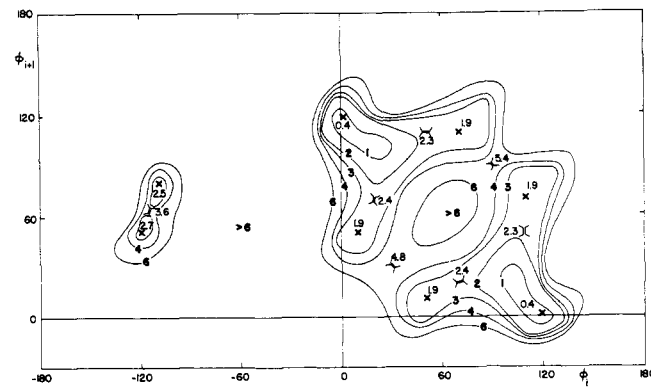

Figure 2. Potential energy contours for bond pair $i,i+1$ of a meso dyad, expressed in kcal mol^{-1} relative to racemic;tt. Methyl rotations χ_{i-1} and χ_{i+1} take on values that minimize the energy for each φ_i,φ_{i+1}. The × denote local minima, and ⟨⟩ denote cols in the surface.

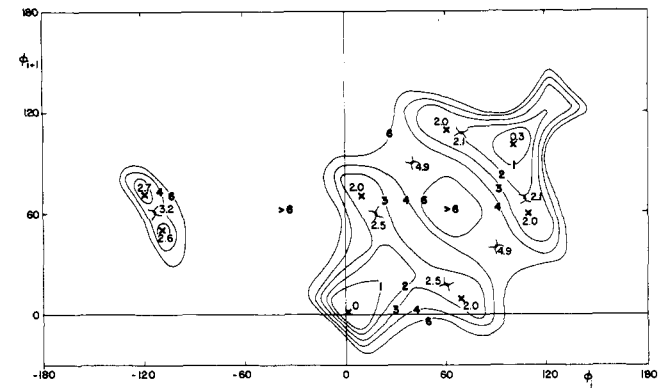

Figure 3. Potential energy contours for bond pair $i,i+1$ of a racemic dyad. See legend to Figure 2.

The torsion angles φ_i and φ_{i+1} are measured according to the convention introduced previously.[13] That is, φ_i in Figure 2, being associated with a *d* bond (see ref 13) as represented in Figure 1, is measured in the right-handed sense relative to the trans position; φ_{i+1}, being associated with a bond of opposite chirality, i.e., with an *l* bond, is measured in the left-handed sense with $\varphi = 0$ for trans. If the configuration of C_{i+1} is inverted by interchanging H and CH_3 connected to C_{i+1}, the resulting dyad is racemic with both skeletal bonds of *d* chirality. The energy surface depicted in Figure 3 corresponds to this dyad, both φ_i and φ_{i+1} being measured in the right-handed sense. Identification of Figure 3 with the racemic enantiomer of *ll* chirality requires that φ_i and φ_{i+1} be measured in the left-handed sense.[13]

Only the "+ +" and "− +" quadrants and the bordering range of φ_{i+1} are shown in Figures 2 and 3. These include the |gg| and |ḡt| domains as well as |tt|, |tg|, and |gt| states, or their displaced counterparts. The vertical lines denote

boundaries of the dyad. The "− −" quadrants, i.e., the quadrants that include the |ḡḡ| domains, may be ignored since the energies there exceed 10 kcal mol^{-1}. The "+ −" quadrants are obtained from "− +" by reflection through the line of $\varphi_i = \varphi_{i+1}$.

The cols between local minima of the energy surfaces are indicated in Figures 2 and 3, together with the energy of the col, in all instances where this energy does not exceed 10 kcal mol^{-1} relative to racemic;tt. The side group rotations χ_{i-1} and χ_{i+1} depart little from the staggered positions for all conformations of low energy; they do not depart therefrom by more than ±20° for any conformation having an energy ≤2 kcal mol^{-1} above the nearest minimum.

The major minima, rounded to the nearest 10° in φ_i and φ_{i+1}, occur at ca. 0,120° (tg) and ca. 120,0° (gt) for the meso dyad and at ca. 0,0°, (tt) and ca. 100,100° (gg) for the racemic. Less favored minima in the "+ +" quadrants occur in pairs of ca. 10,50°, ca. 50,10° (tt) and ca. 70,110°, ca. 110,70° (gg) for the meso dyad, and at ca. 10,70°, ca. 60,110° (tg) and ca. 70,10°, ca. 110,60° (gt) for the racemic, much like the g^+g^- region in *n*-alkanes.[3,9,28] The minima in the "− +" quadrant, and likewise in the "+ −", appear in pairs that are separated by only 20 to 30°. The col between them is low.

The locations of the minima according to our calculations do not differ significantly (ca. ±10°) from those found by Boyd and Breitling,[15] despite differences in the energy functions used. Boyd and Breitling calculated minima only, the character of the energy surfaces in the vicinity of minima and elsewhere being ignored.

Incorporation of the results shown in Figures 2 and 3 in a rotational isomeric state scheme requires allocation of every element of configuration space $(\varphi_i, \varphi_{i+1})$ for which the energy is not excessive to one of the appropriately chosen states. Rational schemes to this end are indicated in Figures 4 and 5. All regions for which $E \leq 6$ kcal mol^{-} relative to racemic;tt are included in the areas demarcated as shown. The dots denote values of the torsional angles averaged over these regions (see Table II below).

The partition function z_ζ, average energy $\langle E \rangle_\zeta$, and averaged rotation angles $\langle \varphi_k \rangle_\zeta$ for each rotational state ζ were calculated according to

$$z_\zeta = \int\int_\zeta \exp(-E/RT)\mathrm{d}\varphi_i \mathrm{d}\varphi_{i+1} \qquad (4)$$

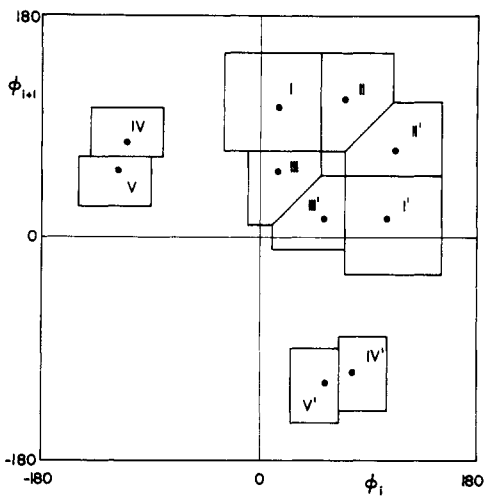

Figure 4. Regions representing isomeric states for a meso dyad. The ● denote averaged angular positions $\langle \varphi_i \rangle, \langle \varphi_{i+1} \rangle$.

$$\langle E \rangle_\zeta = z_\zeta^{-1} \int\int_\zeta E \exp(-E/RT)\mathrm{d}\varphi_i \mathrm{d}\varphi_{i+1} \qquad (5)$$

$$\langle \varphi_k \rangle_\zeta = z_\zeta^{-1} \int\int_\zeta \varphi_k \exp(-E/RT)\mathrm{d}\varphi_i \mathrm{d}\varphi_{i+1} \qquad (6)$$

$$(k = i \text{ or } i + 1)$$

The Boltzman factors were calculated from the energies $E(\varphi_i, \varphi_{i+1})$ at 10° intervals and the integrations were carried out over the regions specified in Figures 4 and 5 using Simpson's rule.

Partition functions z, average energies $\langle E \rangle$, and averaged angles $\langle \varphi_i \rangle$, $\langle \varphi_{i+1} \rangle$ calculated at three temperatures for each of the 11 nonequivalent regions or states in Figures 4 and 5 are listed in Table II. Energies are given relative to E at the minimum for the racemic;tt state. The partition functions are expressed relative to a value of $z = 1$ for this state. The averaged rotation angles are nearly independent of temperature.

Use of the energy function calculated as described above with χ_{i-1} and χ_{i+1} assigned the values that minimize the energy at each conformation implies that the dependence of E on $\chi_{i-1} - \chi_{i-1}^{\min}$ and on $\chi_{i+1} - \chi_{i+1}^{\min}$ is similar for

Table II
Configurational Averages for Dyad Conformation

	z[a]			$\langle E \rangle$,[b] kcal mol^{-1}			$\langle \varphi_i \rangle, \langle \varphi_{i+1} \rangle$, deg		
Region	300 K	400 K	500 K	300 K	400 K	500 K	300 K	400 K	500 K
					Meso				
I	0.7321	0.8028	0.8273	0.94	1.11	1.25	12,108	13,107	14,106
II	0.0512	0.0980	0.1399	2.28	2.42	2.55	71,113	71,111	70,110
III	0.0342	0.0783	0.1245	2.69	2.85	2.98	15,50	16,49	16,48
IV	0.0082	0.0184	0.0284	2.65	2.76	2.87	−110,79	−110,79	−110,79
V	0.0069	0.0181	0.0317	3.05	3.23	3.39	−119,56	−119,55	−119,55
					Racemic				
VI	1.0000	1.0000	1.0000	0.67	0.95	1.19	10,10	12,12	13,13
VII	0.6472	0.6856	0.6978	0.82	1.05	1.25	100,100	100,100	101,101
VIII	0.0350	0.0686	0.1007	2.32	2.51	2.69	58,111	57,111	56,110
IX	0.0329	0.0686	0.1047	2.44	2.66	2.86	13,74	14,75	15,75
X	0.0072	0.0181	0.0295	2.93	3.02	3.11	−120,72	−119,72	−119,72
XI	0.0064	0.0154	0.0252	2.81	2.95	3.10	−110,50	−110,50	−110,49

[a] Expressed in arbitrary units relative to a value of unity for the racemic;tt state, VI. [b] Energies relative to zero for the minimum in the racemic;tt domain, VI.

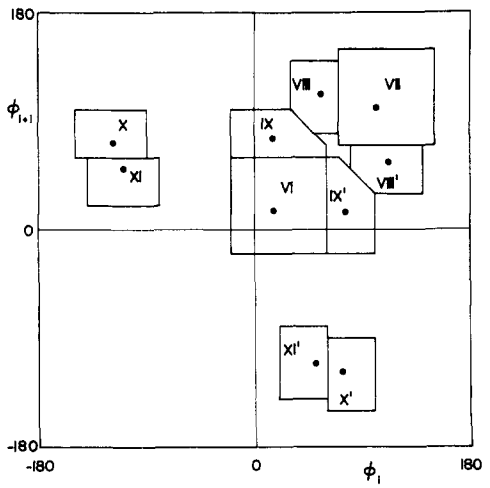

Figure 5. Regions representing isomeric states for a racemic dyad. The ● denote averaged angular positions $\langle\varphi_i\rangle, \langle\varphi_{i+1}\rangle$.

Table III
Increments in z and $\langle E\rangle$ due to Integration over χ's, at 400 K

Region	Δz[a]	$\Delta\langle E\rangle$, kcal mol^{-1}
	Meso	
I	0.344	1.0
II	0.351	0.9
III	0.328	0.8
IV	0.284	0.6
V	0.415	1.0
	Racemic	
VI	0.284	1.1
VII	0.358	0.9
VIII	0.358	0.9
IX	0.351	0.8
X	0.421	0.9
XI	0.284	0.9

[a] Expressed in arbitrary units relative to a value of unity for the racemic;tt state, VI.

all principal states (χ^{min} being the value of χ that minimizes E for particular values of φ_i, φ_{i+1}). Integration over φ_i, φ_{i+1}, χ_{i-1} and χ_{i+1} can then be approximated by integration over φ_i and φ_{i+1} alone, provided that the χ's are equated to the values χ^{min} for every conformation. The error associated with replacement of $E(\varphi_i,\varphi_{i+1},\chi_{i-1},\chi_{i+1})$ by $E(\varphi_i,\varphi_{i+1})$ was ascertained by calculating the contributions $\Delta\langle E\rangle_\zeta$ and Δz_ζ to $\langle E\rangle_\zeta$ and z_ζ from rotations of the side groups when φ_i and φ_{i+1} are assigned their averaged values for each of the 11 nonequivalent domains. The integrations were performed by taking energies at 10° intervals in χ_{i-1} and χ_{i+1}. The increments thus calculated and given in Table III for 400 K appear to be equal within the limits of reliability of the energy calculations. The variations do not exceed the uncertainties in the quantities in Table II. This finding is supported by the observation that graphs of the energy as a function of $\chi_k - \chi_k^{min}$ ($k = i - 1$ or $i + 1$) are virtually superposable for the various minima up to energies of 2 kcal mol^{-1}; appreciable differences appear only above 4 kcal mol^{-1} relative to the minima. We conclude therefore that the disregard of the integration over the χ's in the evaluation according to eq 4, 5, and 6 of the quantities given in Table II is legitimate.

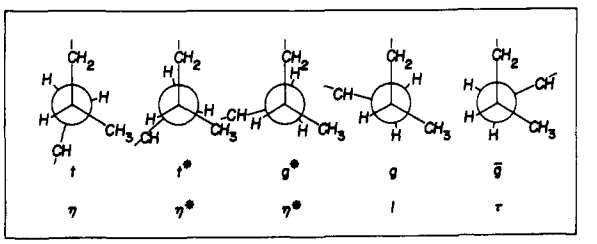

Figure 6. Newman projections along bond i illustrating the basic first-order interactions.

Separation of the backbone conformational energy from that of the side chain rotations in the foregoing manner may not be permissible for vinyl polymers with less symmetrical side groups.[29]

Statistical Weights

Each of the regions in Figures 4 and 5 may be represented by a combination of rotational isomeric states centered at 15, 50, 70, 105, and −115° (compare Table II). We denote these states by t, t*, g*, g, and ḡ, respectively.[1,30] The statistical weights corresponding to the first-order interactions (i.e., those determined by rotation about one bond only) of the five states are indicated in Figure 6. For the two nearly eclipsed conformations, t* and g*, the same statistical weight is assigned, since the dominant interactions between the mutually eclipsing groups, i.e., H and CH, CH_2 and H, CH_3 and H, are very nearly equal.

The same statistical weight ω may be used for all second-order interactions between the pairs of groups CH_2 and CH_2, CH_3 and CH_2, CH_3 and CH_3 separated by four C–C bonds. As may easily be established by examination of models, these interactions are virtually identical in all states in which they occur, except where one of the bonds of the dyad is ḡ. Here the steric overlap is slightly greater,[3] but the difference is insignificant since these states are of rare occurrence and the error can be compensated by a small change in the first-order interaction parameter τ. Furthermore, these interactions need not be distinguished,[29] since the energy surfaces over χ_{i-1},χ_{i+1} are similar for all accessible conformations (cf. above and Table III).

The features of the conformation energy surfaces in Figures 2 and 3 up to at least 6 kcal mol^{-1} above the racemic;tt minimum are well represented by the statistical weight matrices[3,8,13]

$$\mathbf{U}_m'' = \begin{bmatrix} 0 & \eta\eta^*\omega & 0 & \eta & 0 \\ \eta\eta^*\omega & 0 & 0 & 0 & \eta^*\tau\omega \\ 0 & 0 & 0 & \eta^*\omega & \eta^*\tau\omega \\ \eta & 0 & \eta^*\omega & 0 & 0 \\ 0 & \eta^*\tau\omega & \eta^*\tau\omega & 0 & 0 \end{bmatrix} \quad (7)$$

$$\mathbf{U}_r'' = \begin{bmatrix} \eta^2 & 0 & \eta\eta^*\omega & 0 & 0 \\ 0 & 0 & 0 & \eta^*\omega & \eta^*\tau\omega \\ \eta\eta^*\omega & 0 & 0 & 0 & \eta^*\tau\omega \\ 0 & \eta^*\omega & 0 & 1 & 0 \\ 0 & \eta^*\tau\omega & \eta^*\tau\omega & 0 & 0 \end{bmatrix} \quad (8)$$

where the elements are indexed in the order t, t*, g*, g, ḡ. Statistical weights for the |ḡḡ| conformations are set equal to zero on the grounds that they involve excessive steric overlaps, as is readily apparent from inspection of models. Strict adherence to the present scheme would dictate a statistical weight $\tau^2\omega^2$, which is quite negligible.

The foregoing energy calculations, and the statistical weight matrices $\mathbf{U}_m''$ and $\mathbf{U}_r''$, comprehend all first-order

interactions and the second-order interactions dependent upon the rotations for the pair of skeletal bonds *within* a dyad. They take no account of second-order interactions dependent upon rotations about the pair of bonds *flanking* a dyad, e.g., bond pair $i-1,i$ in Figure 1. The statistical weight matrix[3,8] $\mathbf{U}'$ for this latter pair must therefore represent second-order interactions only,[13] all first-order interactions having been included in $\mathbf{U}_m''$ and $\mathbf{U}_r''$.

Significant interactions precipitated by a pair of rotations typified by $\varphi_{i-1}|\varphi_i$, and hence of a second order, occur only for the conformations g|g, ḡ|ḡ, g*|g, g|g*, and g*|g*. The *first two combinations* (involving rotations $g^{\pm}g^{\mp}$ of opposite senses) impose overlaps on the pair of CH groups separated by four bonds, e.g., on groups $i-3$ and $i+1$ in the continuation of the sequence shown in Figure 1; the H-atom centers are at a distance <1 Å. Hence, statistical weights of zero are appropriate for these two combinations.

In the g*|g and g|g* conformations the pendant CH groups cited above are sufficiently separated to alleviate most of the steric repulsion operative in the g|g and ḡ|ḡ conformations. However, at least one of the groups attached to one of these substituted carbons, i.e., to skeletal atom $i-3$ or $i+1$, overlaps the other CH for any combination of *accessible* conformations of the pair of adjoined dyads. For the g*|g pair within a meso–meso triad, for example, these accessible conformations are |gg*|gt|, |gg*|gg*|, |ḡg*|gt|, and |ḡg*|gg*|, as follows from $\mathbf{U}_m''$ according to eq 7. In the first two, $(CH_2)_{i-4}$ overlaps the domain of $(CH)_{i+1}$ excessively, the distance between these C atoms separated by five C–C bonds being 3.0 Å. The H atom on $(CH)_{i+1}$ is separated from C_{i-4} by only 2.1 Å. Corresponding steric overlaps occur in the third and fourth conformations, with $(CH_3)_{i-3}$ replacing $(CH_2)_{i-4}$ as the interferring group.

For a meso–meso triad with central bond pair g*|g*, the conformations otherwise accessible to the adjoined dyads are |gg*|g*ḡ|, |gg*|g*g|, (and its inverse), and |ḡg*|g*ḡ|. These entail steric overlaps even more severe than those for g*|g. For example, in the first of these the centers of the groups $(CH_2)_{i-4}$ and $(CH_2)_{i+2}$ separated by six C–C bonds are at a distance of only 2.6 Å.

Similar steric overlaps occur for other stereochemical configurations of the triad, namely, for meso–racemic and for racemic–racemic, when the central bond pair is either g*|g, g|g*, or g*|g*. The relevant conformations are readily identified by reference to $\mathbf{U}_m''$ and $\mathbf{U}_r''$ as given by eq 7 and 8. Correspondences with the conformations cited above for the meso–meso triad are easily established by appropriate interchanges of CH_3 and CH_2 groups.

Energies associated with the inter-dyad steric overlaps of long range (spanning five or six C–C bonds) in the conformations identified above are in excess of 15 kcal mol^{-1}. Hence, assignment of statistical weights of zero for g*|g, g|g*, and g*|g* is clearly indicated. It is to be noted that these steric repulsions are in addition to those occurring within at least one of the adjoined dyads, and represented by the statistical weight ω in $\mathbf{U}_m''$ and $\mathbf{U}_r''$. The matrix of second-order statistical weights appropriate for the inter-dyad bond pair therefore takes the form

$$\mathbf{U}' = \begin{bmatrix} 1 & 1 & 1 & 1 & 1 \\ 1 & 1 & 1 & 1 & 1 \\ 1 & 1 & 0 & 0 & 1 \\ 1 & 1 & 0 & 0 & 1 \\ 1 & 1 & 1 & 1 & 0 \end{bmatrix} \tag{9}$$

We observe that η^* and ω occur only as the product $\eta^*\omega$ in eq 7 and 8. We therefore replace them by a single parameter, ω^*, that has a mixed first- and second-order character, and write eq 7 and 8 as follows:

Table IV
Conformational Parameters from Energy Calculations

	300 K	400 K	500 K	0 K (extrapolated)
E_η, cal mol^{-1}	40	60	80	0
E_τ, cal mol^{-1}	450	410	390	500
E_{ω^*}, cal mol^{-1}	1640	1600	1580	1700
η_0	1.14	1.18	1.21	1.0 to 1.1
τ_0	0.41	0.39	0.38	0.4 to 0.5
ω_0^*	0.77	0.73	0.72	0.8 to 0.9

Table V
Comparison of Average Energies and Partition Functions from the Three Primary Parameters with Those Obtained Directly from the Conformational Energies

	$\langle E\rangle$,[a] kcal mol^{-1}		z[b]	
Region	Calcd from Table IV	From Table II	Calcd from Table IV	From Table II
I	1.04	1.11	0.819	0.803
II	2.58	2.42	0.074	0.098
III	2.64	2.85	0.081	0.078
IV	2.99	2.76	0.017	0.018
V	2.99	3.23	0.017	0.018
VI	1.10	0.95	0.895	1.000
VII	0.97	1.05	0.750	0.686
VIII	2.58	2.51	0.074	0.069
IX	2.64	2.66	0.081	0.069
X	2.99	3.02	0.017	0.018
XI	2.99	2.95	0.017	0.015

[a] Energies relative to zero for the minimum in the racemic;tt domain, VI. [b] Expressed in arbitrary units relative to a value of unity in the racemic;tt state, VI.

$$\mathbf{U}_m'' = \begin{bmatrix} 0 & \eta\omega^* & 0 & \eta & 0 \\ \eta\omega^* & 0 & 0 & 0 & \tau\omega^* \\ 0 & 0 & 0 & \omega^* & \tau\omega^* \\ \eta & 0 & \omega^* & 0 & 0 \\ 0 & \tau\omega^* & \tau\omega^* & 0 & 0 \end{bmatrix} \tag{10}$$

$$\mathbf{U}_r'' = \begin{bmatrix} \eta^2 & 0 & \eta\omega^* & 0 & 0 \\ 0 & 0 & 0 & \omega^* & \tau\omega^* \\ \eta\omega^* & 0 & 0 & 0 & \tau\omega^* \\ 0 & \omega^* & 0 & 1 & 0 \\ 0 & \tau\omega^* & \tau\omega^* & 0 & 0 \end{bmatrix} \tag{11}$$

The conformational energies E_η, E_τ, and E_{ω^*} can now be determined from the one-to-one correspondence between matrix elements and entries for $\langle E\rangle$ in Table II. Let ξ denote any one of the statistical weights (i.e., η, τ, or ω^*). The index ζ will denote one of the 11 nonequivalent regions identified by I to XI in Figures 4 and 5; it serves as a generic index for a pair of subscripts, e.g., tt. Solution of the over-determined set of 11 linear equations

$$\Sigma E_\xi - \langle E\rangle_\zeta = 0 \tag{12}$$

where the $\langle E\rangle_\zeta$ are taken from Table II and the sum comprises the combination of energies E_ξ contributing to conformation ζ, yields the results listed in Table IV. Letting

$$\xi = \xi_0 \exp(-E_\xi/RT) \tag{13}$$

for each statistical weight ξ, we find the ξ_0 by solving the overdetermined set of 11 linear equations

$$\Sigma \ln \xi_0 - \ln z_\zeta - (\Sigma E_\xi)/RT = 0 \quad (14)$$

since the z_ζ can be identified with the ζ element in the statistical weight matrices $\mathbf{U}''$. The E_ξ are taken from Table IV, the z_ζ from Table II. Results are given in the lower portion of Table IV. The rounded values for energies in the last column were obtained by linear extrapolation to 0 K. The preexponential factors in the last column are so adjusted that, in combination with the energies also given in the last column, they yield values of η, τ, and ω^* valid at all temperatures within the limits of accuracy of the calculations.

In Table V we compare values for $\langle E \rangle$ and z obtained from the statistical weight parameters in Table IV with the results of direct evaluation from the conformational energies (see Table II) for each of the 11 dyad conformations. These comparisons refer to a temperature of 400 K. Root-mean-square differences for the energies are 0.15 kcal mol^{-1}; those for the partition functions amount to 12%.

In recognition of the limitations of the conformational energy calculations,[1,7] we must point out that the energy differences between states depend appreciably on the choice of parameters used in the calculations, i.e., on the values chosen for the bond angles and the van der Waals radii. The preexponential factors, which reflect the shapes of the minima, are quite insensitive to the parameters, however. For this reason, adjustments to achieve agreement with experiment will be confined primarily to the energies.

The parameter τ is of minor importance because it is always associated with at least one factor ω^*. Therefore, E_τ, as well as τ_0, is assigned its calculated value, i.e., we let

$$\tau = 0.4 \exp(-500/RT) \quad (15)$$

with RT expressed in cal mol^{-1}. Average values of the rotation angles given at the beginning of this section have been used in all following calculations.

Stereochemical Equilibrium

We consider vinyl polymers of the general formula

$$H\text{–}(CH_2\text{–}CHR)_x\text{–}CH_3$$

Stereochemical equilibrium and conformational equilibrium are determined by the same set of statistical weight parameters, as shown previously.[2,3] In the case of polypropylene, the identity of the substituent R with the terminal methyl groups renders the terminal dyads symmetric. The previous formulation[2,3] must be revised accordingly. The partition function for the x-meric chain comprising $x - 1$ dyads of which $x - 3$ are subject to diastereoisomerism is conveniently expressed as the following serial product

$$Z = \mathbf{U}_0\mathbf{U}_1^{(2)}\left(\prod_{k=2}^{x-2}\mathbf{U}_k^{(2)}\right)\mathbf{U}_{x-1}^{(2)}\mathbf{U}_x \quad (16)$$

where $\mathbf{U}_k^{(2)}$ is either $\mathbf{U}_m^{(2)} = \mathbf{U}'\mathbf{U}_m''$ or $\mathbf{U}_r^{(2)} = \mathbf{U}'\mathbf{U}_r''$, depending on the stereochemical character of the k-th dyad. The terminal operators are

$$\mathbf{U}_0 = [1, 0, 0, 0, 0] \quad (17)$$

and

$$\mathbf{U}_x = \mathrm{col}(1, 1, 1, 1, 1) \quad (18)$$

The matrices for the terminal dyads 1 and $x - 1$ require special attention. It will be observed that the penultimate bonds are achiral; each joins a terminal isobutyl group. For these bonds the g state is equivalent to t, and g* likewise to t*. The latter two states are assigned the same statistical weights (η^*) in the foregoing scheme. Equivalence of the t and g states for the penultimate bonds is established (see Figure 6) by applying the factor η to the latter state. This is accomplished by defining the matrices for the first and last dyads as follows

$$\mathbf{U}_1^{(2)} = \mathbf{U}'\,\mathrm{diag}(1, 1, 1, \eta, 1)\mathbf{U}'' \quad (19)$$

$$\mathbf{U}_{x-1}^{(2)} = \mathbf{U}'\mathbf{U}''\,\mathrm{diag}(1, 1, 1, \eta, 1) \quad (20)$$

where it is immaterial whether $\mathbf{U}''$ is identified with $\mathbf{U}_m''$ or $\mathbf{U}_r''$ since

$$\mathbf{U}_0\mathbf{U}'\,\mathrm{diag}(1, 1, 1, \eta, 1)\mathbf{U}_m'' \equiv \mathbf{U}_0\mathbf{U}'\,\mathrm{diag}(1, 1, 1, \eta, 1)\mathbf{U}_r'' \quad (21)$$

and

$$\mathbf{U}_m''\,\mathrm{diag}(1, 1, 1, \eta, 1)\mathbf{U}_x \equiv \mathbf{U}_r''\,\mathrm{diag}(1, 1, 1, \eta, 1)\mathbf{U}_x \quad (22)$$

The sum of the values for Z for every stereochemical configuration of the chain as a whole[2,3] is

$$Z = \mathbf{U}_0\mathbf{U}_1^{(2)}\mathfrak{U}^{x-3}\mathbf{U}_{x-1}^{(2)}\mathbf{U}_x \quad (23)$$

where $\mathfrak{U} = \mathbf{U}_m^{(2)} + \mathbf{U}_r^{(2)}$. The fraction of dyads which are meso at equilibrium is given by

$$f_m = (x - 3)^{-1}Z^{-1}[\mathbf{U}_0 0]\hat{\mathfrak{u}}_1\hat{\mathfrak{U}}^{x-3}\hat{\mathfrak{u}}_{x-1}\begin{bmatrix}0\\ \\ \mathbf{U}_x\end{bmatrix} \quad (24)$$

where

$$\hat{\mathfrak{U}} = \begin{bmatrix}\mathfrak{U} & \mathbf{U}_m^{(2)}\\ 0 & \mathfrak{U}\end{bmatrix} \quad (25)$$

$$\hat{\mathfrak{u}}_1 = \begin{bmatrix}\mathbf{U}_1^{(2)} & 0\\ 0 & \mathbf{U}_1^{(2)}\end{bmatrix} \quad (26)$$

$$\mathfrak{u}_{x-1} = \begin{bmatrix}\mathbf{U}_{x-1}^{(2)} & 0\\ 0 & \mathbf{U}_{x-1}^{(2)}\end{bmatrix} \quad (27)$$

The fraction F_I, of isotactic triads (meso–meso) at stereochemical equilibrium, is given similarly[2,3] by

$$F_I = (x - 4)^{-1}Z^{-1}[\mathbf{U}_0 0]\hat{\mathfrak{w}}_{12}\hat{\mathfrak{W}}_I^{x-4}\hat{\mathfrak{w}}_{x-1}\begin{bmatrix}\mathbf{U}_x\\ \\ \mathbf{U}_x\end{bmatrix} \quad (28)$$

where

$$\hat{\mathfrak{w}}_{12} = [\mathfrak{w}_1\mathfrak{w}\ \ 0] \quad (29)$$

$$\hat{\mathfrak{w}}_{x-1} = \begin{bmatrix}0\\ \\ \mathfrak{w}_{x-1}\end{bmatrix} \quad (30)$$

$$\hat{\mathfrak{W}}_I = \begin{bmatrix}\mathfrak{W} & \mathfrak{W}_I'\\ 0 & \mathfrak{W}\end{bmatrix} \quad (31)$$

and

$$\mathfrak{W} = \begin{bmatrix}\mathbf{U}_m^{(2)} & \mathbf{U}_r^{(2)}\\ \\ \mathbf{U}_m^{(2)} & \mathbf{U}_r^{(2)}\end{bmatrix} \quad (32)$$

$$\mathfrak{W}_I' = \begin{bmatrix}\mathbf{U}_m^{(2)} & 0\\ \\ 0 & 0\end{bmatrix} \quad (33)$$

$$\mathfrak{w}_1 = \begin{bmatrix}\mathbf{U}_1^{(2)} & 0\\ \\ 0 & \mathbf{U}_1^{(2)}\end{bmatrix} \quad (34)$$

$$\mathbb{W}_{x-1} = \begin{bmatrix} \mathbf{U}_{x-1}^{(2)} & 0 \\ 0 & \mathbf{U}_{x-1}^{(2)} \end{bmatrix} \quad (35)$$

The fractions of heterotactic (meso–racemic and racemic–meso) and syndiotactic (racemic–racemic) triads, F_H and F_S, are obtained by replacing $\mathbb{W}_I'$ by $\mathbb{W}_H'$ and $\mathbb{W}_S'$, respectively,[2,3] where

$$\mathbb{W}_H' = \begin{bmatrix} 0 & \mathbf{U}_r^{(2)} \\ \mathbf{U}_m^{(2)} & 0 \end{bmatrix} \quad (36)$$

$$\mathbb{W}_S' = \begin{bmatrix} 0 & 0 \\ 0 & \mathbf{U}_r^{(2)} \end{bmatrix} \quad (37)$$

Experimental results for the stereochemical equilibrium in tetrameric ($x = 4$) and pentameric ($x = 5$) homologs, these being the first two members of the series that have diastereomers, have been reported by Suter, Pucci, and Pino.[4,5] Values of f_m for the tetramer 2,4,6,8-tetramethylnonane, obtained at six temperatures from −75 to 290°C, are treated below according to eq 24.

A first estimate of E_η and η_0 can be obtained directly from the experimental value $f_m = 0.459$ at −75°C for $x = 4$, since $\omega^* \ll 1$ at this temperature. With $\omega^* = 0$ the statistical weight matrices reduce to

$$\mathbf{U}_m'' = \begin{bmatrix} 0 & \eta \\ \eta & 0 \end{bmatrix} \quad (38)$$

$$\mathbf{U}_r'' = \begin{bmatrix} \eta^2 & 0 \\ 0 & 1 \end{bmatrix} \quad (39)$$

$$\mathbf{U}' = \begin{bmatrix} 1 & 1 \\ 1 & 0 \end{bmatrix} \quad (40)$$

with $\mathbf{U}_0 = [1,0]$, $\mathbf{U}_x = \text{col}(1,1)$, and $\text{diag}(1,\eta)$ replacing $\text{diag}(1,1,1,\eta,1)$ in eq 19 and 20. It follows that

$$f_m = 2(1 + \eta)/(2 + \eta)^2 \quad (41)$$

for all $x \geq 4$, subject, of course, to the approximation that $\omega^* = 0$. From the experimental result at −75° we obtain $\eta \approx 0.8$. This corresponds to a conformational free energy of ca. 90 cal mol^{-1} at −75°C. Choice of η_0 immediately yields a value for E_η and vice versa.

For a comprehensive evaluation of the parameters involved in eq 24, we first assign τ_0 and E_τ their values given in eq 15. Other parameters are then adjusted to achieve agreement with the experimental results for $x = 4$ over the range of temperature by minimizing the sum of the squares of the differences between f_m and all 51 individual data points[5] using a well-known procedure.[27] In this way we obtain

$$\eta = 1.05 \exp(-70/RT)$$
$$\omega^* = 0.90 \exp(-1500/RT) \quad (42)$$

with RT expressed in cal mol^{-1}. The independent uncertainty limits are less than ±0.05 for the preexponential factors and less than ±10 cal mol^{-1} and ±100 cal mol^{-1} for E_η and E_{ω^*}, respectively, at a confidence level of about 95%. Mutual adjustment of parameters admits wider ranges, however. If one of the four parameters is held constant at an arbitrary value, the experimental results can be matched closely by adjusting the other three. Figures 7 and 8 show the responses of E_η, E_{ω^*}, and one of the preexponential factors to changes in the other preexponential factor, the combination of parameters being required to reproduce the experimental results for $x = 4$. The experimental data cannot be reproduced satisfactorily by eq 24 for any value of $\eta_0 > 1.2$, at which point the curves in Figure 8 are terminated. No corresponding limit was found for smaller values of η_0; none was found for ω_0^* at either extreme in Figure 7.

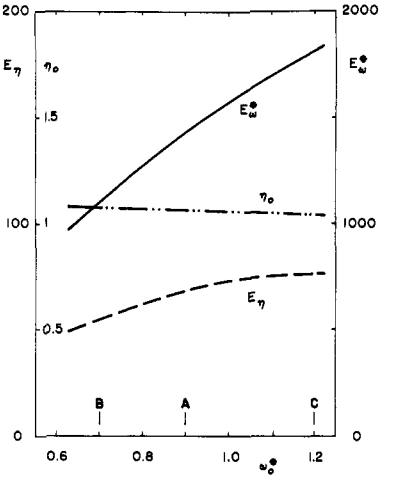

Figure 7. Values for E_{ω^*}, E_η, and η_0 required to fit epimerization results plotted against ω_0^*. Vertical lines above the lower abscissa locate the parameter sets A, B, and C.

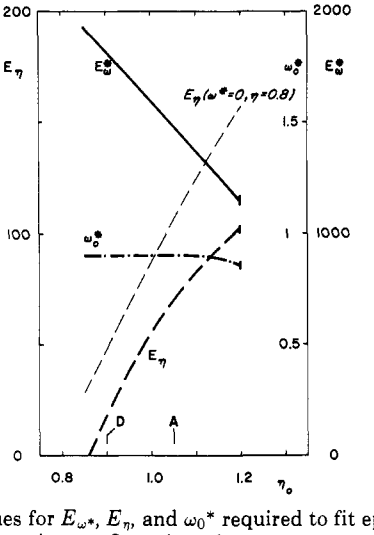

Figure 8. Values for E_{ω^*}, E_η, and ω_0^* required to fit epimerization results plotted against η_0. Location of parameter sets A and D are indicated. The thin broken line shows E_η as a function of η_0 for $\eta = 0.8$ and $\omega^* = 0$.

Figure 8 includes an additional curve for E_η as a function of η_0 according to eq 41 for $\omega^* = 0$ with $F_m = 0.459$ at −75°C (see above). The difference between E_η thus estimated and E_η according to eq 24, given by the lowermost curve in Figure 8, is comparatively small. It will be apparent that eq 41 affords a fairly good estimate of η from the stereochemical equilibrium at low temperatures.

The preexponential factors in the overall best parameter set (eq 42) are remarkably close to those estimated from conformational energies and given in Table IV (last column). Figures 7 and 8 show, however, that a close fit can also be obtained from parameter sets with other values of the preexponential factors. For further calculations, we therefore chose four parameter sets arbitrarily from Figures 7 and 8. These are indicated in the figures and are given numerically in Table VI. The four sets span the admissible ranges of the parameters that are compatible with the energy calculations. Values of f_m calculated according

Table VI
Representative Sets of Conformational Parameters[a] Chosen to Fit Experimental Stereochemical Equilibrium for $x = 4$

Set	E_η	E_τ	E_{ω^*}	η_0	τ_0	$\omega_0{}^*$
A	70	500	1500	1.05	0.4	0.9
B	60	500	1200	1.07	0.4	0.7
C	75	500	1800	1.04	0.4	1.2
D	20	500	1800	0.90	0.4	0.9

[a] Energies are expressed in cal mol^{-1}.

Table VII
Calculated and Experimental Values for F_I, F_S, F_H, and f_m for $x = 5$ at 270°C

Set	f_m	F_I	F_S	F_H
A	0.485	0.234	0.264	0.502
B	0.484	0.233	0.265	0.502
C	0.485	0.234	0.265	0.502
D	0.485	0.233	0.264	0.503
Expt[a]	0.487 ± 0.003	0.237 ± 0.002	0.263 ± 0.002	0.500 ± 0.002

[a] Reference 4; the error limits are standard deviations.

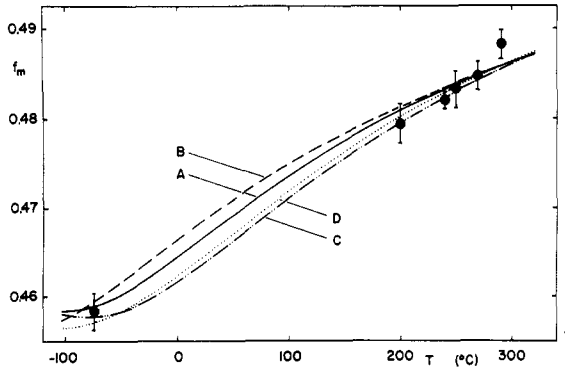

Figure 9. Fraction f_m of meso dyads in the tetramer ($x = 4$) at stereochemical equilibrium plotted against temperature. The curves correspond to the indicated parameter sets. The filled circles denote experimental values from ref 4; error bars show the standard deviations of the experimental data.

to eq 24 for each set of parameters are plotted against temperature in Figure 9. Set A affords the best fit (compare eq 42).

Values for F_I, F_S, and F_H for $x = 5$ calculated for $T = 270$°C from each set of parameters using the equations given above are compared in Table VII with the experimental results for 2,4,6,8,10-pentamethylundecane.[4,5] The agreement is good for all parameter sets. The values of f_m also are uniformly in close agreement with observation. The fact that the f_m for $x = 4$ and for $x = 5$ are nearly equal at the same temperature (calcd: 0.484 and 0.485 for $x = 4$ and 5, respectively, compared with observed values of 0.485 ± 0.002 and 0.487 ± 0.003) indicates the trend with chain length to be very small. This conjecture is confirmed by calculations for $x > 5$.

Characteristic Ratios

The characteristic ratio $C_n = \langle r^2 \rangle_0 / nl^2$ was calculated according to well-known methods[3,8,9,13] using the five-state scheme formulated on the basis of the potential energy calculations in conjunction with geometric parameters given above. Figure 10 shows the dependence of C_n on the fraction w_m of meso dyads, calculated using each of the four sets of parameters identified in Table VI. Calculations were carried out for chains of 200 bonds ($x = 100$). Those for the extremities of the plot, $w_m = 0$ and 1, are exact. For intermediate values of w_m, Monte Carlo chains were generated with Bernoullian distributions of meso and racemic dyads. Five chains of 200 bonds were generated at each intermediate value of w_m, the same set of five chains being used for all parameter sets (i.e., sets A through D from Table VI). The continuous curve represents results of calculations carried out with parameter set A for a temperature of 140°C at all stereochemical compositions. Points and bars indicating standard deviations are included for this curve only. In order to facilitate comparison with experiment, the temperature in all other calculations was altered according to the range of the tacticity parameter w_m, as indicated in Figure 10. Extension of the calculations for stereoregular syndiotactic and isotactic chains to larger values of x as required to achieve convergence of the characteristic ratio to its limit C_∞ yielded values which exceed those in Figure 10 by less than 0.5 and 0.1, respectively (i.e., for parameter set D, $C_\infty = 13.8$ at 50°C for $w_m = 0$ and $C_\infty = 5.5$ at 140°C for $w_m = 1$). Abe[31] has shown that C_n for atactic chains approaches its limit more rapidly than for stereoregular ones. Hence, chains of $n = 200$ bonds used in the calculations are of sufficient length to warrant identification of the characteristic ratio C_n with its asymptotic limit.

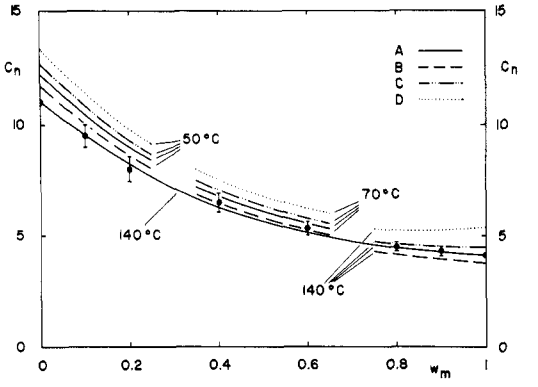

Figure 10. The mean characteristic ratios for Monte Carlo chains of 200 bonds. The curves are calculated for the four parameter sets (see inset) at the three temperatures indicated. The continuous solid line is for set A at 140°C. Averages for five Monte Carlo chains at 140°C are denoted by ●. The error bars represent standard deviations. All calculations were carried out using the five-state scheme defined in the text.

The curves in Figure 10 for the different sets of parameters are similar, apart from being displaced somewhat from one another. In their principal features they resemble previous calculations carried out with the three-state model.[6,30,31] The dependence of C_n on stereoregularity is strongest in the syndiotactic range. The values for C_n decrease monotonically as the portion of meso dyads, w_m, increases. The dependence of C_n on stereoregularity decreases simultaneously and is small in the isotactic range, where the values are somewhat lower than were calculated previously using the three-state scheme. Thus, according to these calculations, the presence of 5 to 10% of racemic dyads should have little effect on C_n for predominantly isotactic chains.[1,33–35] The present calculations exhibit the characteristics typical of chains with large deviations of the preferred rotation angles from locations for perfect staggering.[8,29–32]

Experimental results on the unperturbed dimensions of polypropylenes of various stereochemical compositions are assembled in Table VIII from the sources indicated. Com-

Table VIII
Experimental Values of Characteristic Ratios and Temperature Coefficients of Unperturbed Dimensions of Polypropylenes

Stereoregularity	$\langle r^2\rangle_0/nl^2$	Ref	-10^3d ln $\langle r^2\rangle_0$/dT, K^{-1}	Ref
Isotactic	6.4 (125°C)	*a*	*ca.* 4	*a*
	5.9 (143°C)	*a*	≤1.5	*f*
	5.8 (145°C)	*b*		
	4.7 (145°C)	*c*		
	5.0 (183°C)	*a*		
Atactic	6.8 (34°C)	*d*	*ca.* 0.1	*d*
	7.2 (74°C)	*d*		
	6.9 (92°C)	*d*		
	5.4 (153°C)	*d*		
Syndiotactic	6.7 (45°C)	*e*	*ca.* 1	*e*

[a] A. Nakjima and A. Saijyo, *J. Polym. Sci., Part A-2*, 6, 735, (1968). [b] J. B. Kinsinger and R. E. Hughes, *J. Phys. Chem.*, 63, 2002 (1959). [c] F. Heatley, R. Salovey, and F. A. Bovey, *Macromolecules*, 2, 619 (1969). [d] J. B. Kinsinger and R. E. Hughes, *J. Phys. Chem.*, 67, 1922 (1963). [e] H. Inagaki, T. Miyamoto, and S. Ohta, *ibid.*, 70, 3420 (1966). [f] F. Hamada, unpublished.

parison of the results for isotactic polymers with the calculations shown in Figure 10 shows all parameter sets to be acceptable, with the possible exception of set B. Similarly, the characteristic ratios calculated for atactic chains, using each of the four sets of parameters, agree satisfactorily with experimental values. The significance of the latter suffer from the lack of definitive information on the stereostructure of the polymers investigated.[36,37]

For the syndiotactic polymers we calculate $11 < C_n < 13.5$ for $w_m = 0$ compared with an experimental value of 6.7.[38] Since the stereoregularity of the "syndiotactic" polymer used in the cited investigation is not known,[38,39] the apparent discrepancy may not be as serious as would at first appear. Moreover, a recent investigation of the structure of "syndiotactic" polypropylenes indicates the presence of a substantial fraction of head-to-head/tail-to-tail placements,[40] a fact that further obscures the comparison. We conclude that experimental evidence at hand does not contradict the theoretical value for C_n for syndiotactic polypropylene chains.

Calculated temperature coefficients d ln $\langle r^2\rangle_0$/dT of the chain dimensions, or of the characteristic ratios, are shown in Figure 11. The curves were drawn from averages calculated for five chains of 200 bonds each. Points and standard deviations are shown only for parameter set A. All four sets give similar values for syndiotactic and stereoirregular chains, while in the isotactic region sets C and D produce larger values than sets A and B. Hamada's[41] experimental value, $-\text{d ln}\langle r^2\rangle_0/\text{d}T \leq 1.5 \times 10^{-3}$ K^{-1} (see Table VIII), for isotactic polypropylene probably is the most reliable one available.[31,35] It is well reproduced by the parameter sets A and B. However, in view of experimental inaccuracies and the undetermined degrees of stereoregularity in the samples investigated, none of the parameter sets can be set aside on this basis alone. Temperature coefficients calculated for atactic chains (Figure 11) are in good agreement with the observed value listed in Table VIII, if the uncertainties pertaining to the experimental value are duly recognized. Comparison of theory and experiment for syndiotactic chains is futile for the reasons pointed out above.

Although agreement with the available experimental results can be judged satisfactory for all of the sets of parameters, set A appears to be preferable. Other sets tend either

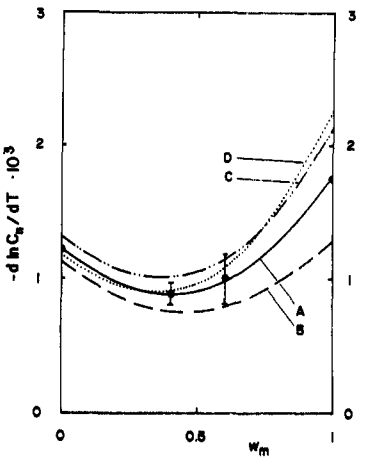

Figure 11. The temperature coefficient of the characteristic ratio for Monte Carlo chains with 200 bonds. The curves correspond to the indicated parameter sets. Filled circles denote averages of five chains with error bars representing standard deviations for set A.

to yield values of C_n that are too low for isotactic chains (e.g., set B) or a temperature coefficient whose magnitude is too great (e.g., sets C and D).

Conclusions

The five-state scheme inferred from the conformational energy calculations stands in full agreement with results of experiment. Foremost among the latter are those obtained from stereochemical equilibration of short homologs of polypropylene[4,5] which afford a quantitative test of theory. Such experimental results depend only on the statistical weights and not on the location of conformational domains or of the rotational isomeric states chosen to represent them. Chain dimensions and their temperature coefficients depend on the latter as well as on the statistical weights, but are known with less accuracy from experimental results currently available. Within the limits of uncertainties in the experimental results, however, the theoretical treatment according to the five-state scheme appears to be well supported by these results.

The set of parameters affording best agreement with experiment, i.e., set A, matches the deductions obtained directly from the energy calculations (compare Tables IV and VI). The agreement may be partially fortuitous; whereas the predictions of the angles specifying the mean locations for the respective domains are considered to be reliable, the relative partition functions and particularly the relative (mean) energies of these domains are subject to error stemming from uncertainties in the parameters entering into the energy calculations. In general, adjustments in the relative energies of states should be anticipated to be required in order to achieve agreement with experiment. The fact that such adjustments seem not to be necessary in the case of polypropylene is gratifying, but perhaps fortuitous in part.

Be this as it may, the parameters given in eq 42 should be rounded to

$$\begin{aligned} \eta &= 1.0 \exp(-60/RT) \\ \tau &= 0.4 \exp(-500/RT) \\ \omega^* &= 0.9 \exp(-1600/RT) \end{aligned} \tag{43}$$

with RT in cal mol^{-1}. The more precise figures in eq 42 were adopted for the purpose of comparing calculations with different parameter sets. The adjustment of rotation angles from their averaged values for the various domains (see Table II), as required for the selection of a unique set

of rotational isomeric states, entails a further approximation. The error incurred is believed to be small.

The mean values of the rotation angles in the principal domains depart appreciably from the locations of minima (compare averaged angles in Table II with locations of the minima marked in Figures 2 and 3). Moreover, the shapes of the domains, reflected in the products of factors ξ_0 for the given domain, differ considerably. It is apparent that identification of rotational isomeric states with the minima would risk substantial error.

The three-state scheme used previously also can be fitted to the experimental data through suitable choice of parameters.[4-6] It has long been known that the actual pattern of energy domains departs from this simplified model,[3,8] but with suitable adjustments of statistical weights in recognition of these departures, the experimental results currently available can be reproduced satisfactorily. With respect to calculations of characteristic ratios, the principal difference between the three- and the five-state schemes occurs in the dependence of C_∞ on w_m in the syndiotactic range; calculations according to the five-state scheme indicate a greater increase in C_∞ as $w_m \rightarrow 0$ (see Figure 10).

The five-state scheme appears not to be rigorously reducible to one of three states. A qualitative correspondance to a three-state scheme may be traced, however. To this end, let the t* state ($\varphi = 50°$) be combined with t ($\varphi = 15°$) and let the g* state ($\varphi = 70°$) be combined with g ($\varphi = 105°$); the $\bar{g}$ state ($\varphi = 115°$) remains intact. The principal conformations, namely, tg(I) and gt(I′) for meso and tt(VI) and gg(VII) for racemic, are unaffected by the reduction to three states. For the meso dyad, the conformations g*g (II) and gg*(II′) are merged to yield a coalesced gg conformation displaced somewhat from the mean position of the two conformations thus combined (see Figure 4). The tt*(III) and t*t(III′) conformations are similarly merged and relocated. One of the angles in each of the equivalent conformations $\bar{g}g^*$(IV) and $g^*\bar{g}$(IV′) is shifted by 35° in the process of reduction in the stipulated manner. Conformations $\bar{g}t^*$(V) and $t^*\bar{g}$(V′) are shifted similarly. Conformations for the racemic dyad are merged and shifted analogously, as may easily be ascertained. The resulting three-state scheme corresponds to the one proposed a number of years ago by Mark and Abe in collaboration with one of the present authors,[8] and applied subsequently to various monosubstituted vinyl polymers.[3,30-32] Moreover, the locations of the three states deduced from the five-state scheme comply with the rule offered previously according to which

$$\varphi_g = 120° - \varphi_t \qquad \varphi_{\bar{g}} = -120° \tag{44}$$

when transcribed to current conventions[13] pertaining to the specification of rotational states and their angles of rotation.

The foregoing condensation suggests reduction of the 5 × 5 statistical weight matrices by partitioning them in corresponding fashion and adding the statistical weights within each submatrix to form a single element. The resulting 3 × 3 matrices are not algebraically equivalent, however, to the 5 × 5 matrices for the generation of the partition function and other quantities. They are inconsistent also with the statistical weight matrices deduced previously for implementation of the three-state scheme. Thus, the present five-state scheme does not lend itself to algebraic reduction to an acceptable three-state scheme, and hence is formally unrelated in this sense to the latter.

In summary, existing experimental results bearing on the configurational statistics of the polypropylene chain can be represented satisfactorily by a three-state model. It does not appear feasible, however, to relate this model rigorously to the pattern of the conformational energy that characterizes the polypropylene chain, which clearly calls for five states. From this standpoint, the three-state scheme is unsatisfactory approximation to the actual conformational energy, its empirical success notwithstanding. When more accurate experimental results concerning the spatial configuration are forthcoming, the greater refinement and closer conformance to reality of the five-state model may be required.

Finally, we remark on the persistence of the preferred |tg| or |gt| conformation for an isotactic chain. The preference for this conformation has often been asserted to lead to the prevalence of helical sequences of considerable length when polypropylene is dispersed in a solvent or when melted. The average length of such sequences calculated directly from the parameter set A is only 2.2 monomer units at 400 K. The percentage of units in |tg| and |gt| conformation is 66% of this temperature. At 300 K the average length of a sequence is 2.8 units and 76% of the chain is either |tg| or |gt|. Clearly, representation of the random chain of isotactic polypropylene as a succession of helical sequences is incorrect.

Note Added in Proof. Asakura, Ando, and Nishioka[42] have calculated conformational energies for 2-methylbutane, pentane, 2,4-dimethylpentane, 2,4,6-trimethylheptane and 2,4,6,8-tetramethylnonane by MO methods (CNDO/2). From their calculations for the first two compounds they estimate $E_\tau \approx 0.5$ kcal mol^{-1} and $E_\omega \approx 1.5$ kcal mol^{-1}, in substantial agreement with our results. From their results for the other three compounds the authors conclude, as we do, that the potential surfaces around the most favored minima are asymmetric and that therefore the conformational characteristics cannot be described by the energies at the minima of the potential troughs alone. Also, they obtain torsion angles for these minima in good agreement with our values. While we agree with Asakura et al. that the conventional three-state rotational isomeric scheme is incorrect in its representation of the conformational energy, the five-state scheme here presented is in harmony with their calculations as well as with ours.

Acknowledgment. This work was supported by the Directorate of Chemical Sciences, U.S. Air Force Office of Scientific Research Grant No. AFOSR-73-2441-A-B.

References and Notes

(1) P. J. Flory, *J. Polym. Sci., Polym. Phys. Ed.*, **11**, 621 (1973).
(2) P. J. Flory, *J. Am. Chem. Soc.*, **89**, 1798 (1967).
(3) P. J. Flory, "Statistical Mechanics of Chain Molecules", Interscience, New York, N.Y., 1969.
(4) U. W. Suter, S. Pucci, and P. Pino, *J. Am. Chem. Soc.*, **97**, 1018 (1975).
(5) U. W. Suter, Doctoral Thesis No. 5133, Swiss Federal Institute of Technology, Zürich, 1973.
(6) U. Biskup and H. J. Cantow, *Macromolecules*, **5**, 546 (1972).
(7) P. J. Flory, *Macromolecules*, **7**, 381 (1974).
(8) P. J. Flory, J. E. Mark, and A. Abe, *J. Am. Chem. Soc.*, **88**, 631 (1966).
(9) A. Abe, R. L. Jernigan, and P. J. Flory, *J. Am. Chem. Soc.*, **88**, 631 (1966).
(10) G. Natta, P. Corradini, and P. Ganis, *Makromol. Chem.*, **39**, 238 (1960).
(11) G. Natta, P. Corradini, and P. Ganis, *J. Polym. Sci.*, **58**, 1191 (1962).
(12) N. P. Borisova and T. M. Birshtein, *Vysokomol. Soedin.*, **5**, 279 (1963).
(13) P. J. Flory, P. R. Sundararajan, and L. C. DeBolt, *J. Am. Chem. Soc.*, **96**, 5015 (1974).
(14) The calculations referred to were carried out according to a four-state scheme obtained by incorporating the two additional states mentioned and by deletion of the $\bar{g}$ state. In other respects this model anticipated the five-state scheme presented below, although the locations of the several states departed somewhat from those deduced in this paper.
(15) R. H. Boyd and S. M. Breitling, *Macromolecules*, **5**, 279 (1972).
(16) J. Ketelaar, "Chemical Constitution", Elsevier, New York, N.Y., 1958.
(17) D. A. Brant, W. G. Miller, and P. J. Flory, *J. Mol. Biol.*, **23**, 47 (1967).
(18) J. H. Schachtschneider and R. G. Snyder, *Spectrochim. Acta*, **19**, 117 (1963).

(19) R. G. Snyder and G. Zerbi, *Spectrochim. Acta, Part A*, **23**, 391 (1967).
(20) G. N. Ramachandran and C. M. Venkatachalam, *Biopolymers*, **6**, 1255 (1968).
(21) M. Bixon and S. Lifson, *Tetrahedron*, **23**, 769 (1967).
(22) M. H. Liberman, L. C. DeBolt, and P. J. Flory, *J. Polym. Sci., Polym. Phys. Ed.*, **12**, 187 (1974).
(23) C. W. Bunn and D. R. Holmes, *Discuss. Faraday Soc.*, **25**, 95 (1958).
(24) P. Corradini, "Stereochemistry of Macromolecules", Vol. 3, A. D. Ketley, Ed., Marcel Dekker, New York, N.Y., 1968, p 1.
(25) T. Miyazawa, ref 24, p 147.
(26) D. R. Lide, Jr., *J. Chem. Phys.*, **33**, 1519 (1960).
(27) D. W. Marquardt, *J. Soc. Ind. Appl. Math.*, **11**, 431 (1963).
(28) R. A. Scott and H. A. Scheraga, *J. Chem. Phys.*, **44**, 3054 (1966).
(29) U. Biskup and H.-J. Cantow, *Makromol. Chem.*, **168**, 315 (1973).
(30) Y. Fujiwara and P. J. Flory, *Macromolecules*, **3**, 280 (1970).
(31) A. Abe, *Polym. J.*, **1**, 232 (1970).
(32) A. E. Tonelli, unpublished results.
(33) A. Zambelli, A. Segre, M. Farina, and G. Natta, *Makromol. Chem.*, **110**, 1 (1967).
(34) F. Heatley, R. Salovey, and F. A. Bovey, *Macromolecules*, **2**, 619 (1969).
(35) P. J. Flory, *Macromolecules*, **3**, 613 (1970).
(36) J. B. Kinsinger and R. E. Hughes, *J. Phys. Chem.*, **67**, 1922 (1963).
(37) J. C. Randall, *J. Polym. Sci., Polym. Phys. Ed.*, **12**, 703 (1974).
(38) H. Inagaki, T. Miyamoto, and S. Ohta, *J. Phys. Chem.*, **70**, 3420 (1966).
(39) G. Natta, I. Pasquon, and A. Zambelli, *J. Am. Chem. Soc.*, **84**, 1488 (1962).
(40) K. Mitani, T. Suzuki, A. Matsuo, and Y. Takegami, *J. Polym. Sci., Polym. Chem. Ed.*, **12**, 771 (1974).
(41) F. Hamada, unpublished.
(42) T. Asakura, I. Ando, and A. Nishioka, *Makromol. Chem.*, **176**, 1151 (1975).

Conformational Characteristics of Polystyrene

D. Y. Yoon, P. R. Sundararajan, and P. J. Flory*

Department of Chemistry, Stanford University, Stanford, California 94305.
Received June 16, 1975

ABSTRACT: Conformational energies of meso and racemic dyads of polystyrene have been computed as functions of skeletal bond rotations. Confinement of rotations of the phenyl groups to a small range within which they are nearly perpendicular to the plane defined by the two adjoining skeletal bonds is confirmed. Steric interactions involving the relatively large planar phenyl group virtually preclude $\bar{g}$ conformations. Four prominent minima, denoted tt, gg, tg, and gt, are indicated for both meso and racemic dyads. The energy of the meso;tt state, in which the phenyl groups are apposed and in close proximity, is much reduced by shifts in the torsion angles from 0,0° (for perfect staggering) to 20,20°, the latter being the location of the meso;tt minimum according to the energy calculations. The reduced exposure of the phenyl groups to solvent in the tt conformation of the meso dyad compared to other accessible conformations necessitates revision of the energy calculations to take account of solvent interactions. Apart from alteration of the energy of the meso;tt conformation, the topography of the conformation energy surface is little affected by such revision. A simple, two-state rotational scheme is applicable with states at $\varphi_t = 10°$ and $\varphi_g = 110°$ for both meso and racemic dyads. The first-order interaction parameter η expressing the preference for the t over the g state is given by $\eta = 0.8\ (\pm 0.1)\ \exp(-E_\eta/RT)$ where $E_\eta = -400 \pm 100$ cal mol^{-1}, the preexponential factor being evaluated from the computed conformational energy surface and E_η from stereochemical equilibria in polystyrene oligomers (Williams and Flory). Second-order parameters ω, ω', and ω'' for the interactions CH_2–CH_2, CH_2–C_6H_5 and C_6H_5–C_6H_5, respectively, are evaluated from the present calculations supplemented by adjustments of the energy $E_{\omega''}$ to reproduce the observed characteristic ratio C_∞ for isotactic polystyrene. Calculated values of C_∞ and d ln C_∞/dT for atactic polystyrene are consistent with experimental results.

The polystyrene chain H–[CH_2–$CH(C_6H_5)$–]$_x$$CH_3$ possesses distinctive features that set it apart from polypropylene treated in the preceding paper.[1] The phenyl substituent has a plane of symmetry, whereas the methyl group is quasi-cylindrical. Although it is much larger than methyl in volume, its smaller dimension is less than the diameter of the methyl group. Its steric requirements differ markedly from those of the skeletal CH_2 group which, as noted in the preceding paper,[1] resemble those of the CH_3 group.

As will become apparent from examination of models (see Figure 1), these characteristics of the phenyl group have important consequences as follows.

(i) Owing to the comparatively small thickness of the phenyl group, the severe steric interactions between substituents normally occurring in the tt conformation of a meso dyad of a vinyl chain[2] can be diminished considerably by small displacements of the rotations φ_i and φ_{i+1} from their values (zero) for perfect staggering.

(ii) The proximity of the phenyl groups in this conformation (or in its analog, t$\bar{g}$, for the racemic dyad) limits access of solvent molecules to the polymer chain, and, in particular, to the comparatively large phenyl groups. The energy of interaction between solvent and polymer is, therefore, appreciably dependent on conformation. The effects of this dependence must be taken into account in reckoning the conformational energy.

(iii) The $\bar{g}$ conformation is subject to steric interactions of such severity as to obviate its consideration. (For the definition of g and $\bar{g}$ states, see ref 3 and the preceding paper.) These steric interactions, which are identified and examined in this paper, are analogous to those found likewise to exclude the $\bar{g}$ conformation in poly(methyl methacrylate),[4] wherein one of the substituents, the ester group, is planar and, hence, resembles phenyl in its spatial requirements.

In order to clarify the various interactions in polystyrene chains, we have carried out conformational energy calculations using conventional empirical methods cited in the preceding paper. The solvent interaction energy is taken into account in crude approximation. In recognition of limitations of the energy calculations, we rely on them principally to define the accessible regions of conformational space and the shapes of these domains. The estimated energies are adjusted within reasonable ranges as required to achieve agreement with experimental results on stereochemical equilibria in polystyrene oligomers and on the dimensions of isotactic and atactic polystyrene chains.

Conformational Energies

Geometric Data and Methods of Calculation. Bond lengths and bond angles are given in Table I. The bond an-